

## Electronic Structure and Optical Properties of Dianionic and Dicationic $\pi$ -Dimers

Yuanzuo Li,<sup>†,‡</sup> Huixing Li,<sup>†</sup> Xiuming Zhao,<sup>†</sup> and Maodu Chen<sup>\*,†</sup>

School of Physics and Optoelectronic Technology, and College of Advanced Science and Technology, Dalian University of Technology, Dalian 116024, People's Republic of China, and Beijing National Laboratory for Condensed Matter Physics, Institute of Physics, Chinese Academy of Sciences, P.O. Box 603-146, Beijing, 100190, People's Republic of China

Received: April 9, 2010; Revised Manuscript Received: May 23, 2010

The absorption spectra of dianionic tetrocyanoethylene and dicationic tetrathiafulvalene dimers have been studied theoretically with the time-dependent density functional theory and the recently proposed Coulomb-attenuated model. The nature of the excited states was further explored by means of the two-dimensional (2D) site (transition density matrix) and three-dimensional (3D) cube (transition density and charge difference density) representations. By use of the 3D transition density and charge difference density, we visualized the orientation of transition dipole moment and also explained charge-transfer characteristics occurring in the dianionic/dicationic  $\pi$ -dimers system. It is found that for the dianionic/dicationic  $\pi$ -dimers system there exist two kinds of charge-transfer patterns for the mainly excited states, the intermolecular charge transfer and the mixture of intramolecular charge transfer coupled with intermolecular charge transfer. Meanwhile, the coupling effect of excitation and the oscillation of electron–hole pairs between the monomers have been revealed with 2D site representation of transition density matrix, which also indicates the electron–hole coherence upon photon excitation.

### I. Introduction

Noncovalent interactions are critical for a variety of scientific applications, including protein structure, DNA base-pair stacking, molecular/biomolecular assembly, and functional molecular materials.<sup>1,2</sup> The building blocks of the noncovalent system can interact with each other or with their environment through several interaction modes (such as van der Waals, hydrogen bonding,  $\pi$ – $\pi$  and cation– $\pi$  interactions),<sup>3–9</sup> which constitute the important source of stability and electronic properties. From both fundamental and practical points of view, it is interesting to understand the excited-state properties and charge-transfer mechanism of the charged  $\pi$ -dimers since those dianionic/dicationic  $\pi$ -dimers are widely utilized components in crystalline molecular conductors.<sup>10–19</sup>

Tetrocyanoethylene (TCNE) as an electron acceptor is widely applied in molecular-based electron transfer salts that exhibit properties of technological interest.<sup>11,12,16</sup> Through four-center two-electron intermolecular  $\pi$ -orbital bonding, the two TCNE<sup>–</sup> can form the dianion  $\pi$ -dimers, and the binding orbital of dianion  $\pi$ -dimers will be occupied by excess electrons. While for the configuration of TTF cation radical, spectral evidence indicated that there exists the intrinsic cation radical absorption usually interpreted as a  $\pi$ -dimer band. Considerable efforts have been done to explore the excited-state behavior and charge-transfer dynamics occurring in the charged TTF dimer<sup>13–15</sup> and TCNE dimer.<sup>16–19</sup> There are, however, remarkably few researches on the visualized photoinduced charge transfer (CT) process in the charged dimers, and the knowledge of the coupling effect between the dimer counterparts has been still inadequate.

Several theoretical calculations have also been performed to investigate the structural features and excited states of a

$\pi$ -stacked system.<sup>4,5,20–28</sup> Miller et al. used a hybrid DFT approach to calculate electronic properties of the ground state of the long, multicenter bonding in 7,7,8,8-tetracyano- $p$ -quinodimethane anion radical dimers.<sup>25</sup> Density functional theory (DFT) and time-dependent density-functional theory (TDDFT) calculations on stacked NDA bases were reported by Impronta et al.,<sup>26</sup> whose work provided a clear description of the characteristic states relevant to the different lifetime components evidenced by time-resolved experiments. Recently, Chakrabarti et al. used developed long-range corrected functionals to calculate the absorption spectrum of fullerene-buckycatcher supramolecule and revealed the importance of  $\pi$ -stacked interaction in controlling absorption properties of the objective system.<sup>27</sup> Additionally, intermolecular charge-transfer excitation in ethylene dimer was studied with the developed functionals at the TDDFT level of theory.<sup>28</sup>

In the present paper, quantum chemical calculation as well as visualized real-space analysis has been used to explore the nature of excited state of dianionic TCNE and dicationic TTF dimers (such as transition moment, charge transfer, and coupling effect of excitation). The paper is organized as follows: first, the theoretical approaches are described, and then simulated absorption spectra are compared with the related experiment. Second, the excited-state properties of dianionic TCNE and dicationic TTF are studied with the visualized 2D and 3D real space analyses.<sup>29–35</sup> The 3D cube representation of transition density reveals the orientation of transition dipole moment, and 3D charge difference density indicates the orientation and the result of intermolecular charge transfer during electronic transition,<sup>29,31–35</sup> and the 2D site representation reveals the electron–hole coherence of electron–hole pairs on excitation.<sup>30</sup> A study of CT mechanism and coupling effect occurring in the charged dimers provides detailed insight into the excited state properties of the differently charged dimers.

\* To whom correspondence should be addressed. E-mail: mdchen@dlut.edu.cn. Phone: +86-411-84706101-604.

<sup>†</sup> Dalian University of Technology.

<sup>‡</sup> Chinese Academy of Sciences.

## II. Methods

The dianionic TCNE and dicationic TTF ground-state geometry were fully optimized by means of the DFT<sup>36</sup> at the 6-31G(d) basis set. The optical absorption was calculated by the TD-DFT<sup>37</sup> at the same level. The Coulomb attenuating method B3LYP (CAM-B3LYP),<sup>38</sup> combining the hybrid qualities of B3LYP and the long-range correction, was used in the ground and excited state calculations. All of the above quantum-chemical calculations were performed with the Gaussian 09 suite of programs.<sup>39</sup>

As results from the TD-DFT calculation, the singlet excited states  $|S_n\rangle$  are represented by vectors  $C_{n,ai}^{\text{CI}}$  based on configurations of unoccupied and occupied molecular orbitals  $a$  and  $i$ , respectively. The molecular orbitals are in turn given by linear combinations of atomic orbitals (LCAO)  $\mu$  and  $\nu$  with coefficients  $c_{\mu i}^{\text{LCAO}}$  and  $c_{\nu i}^{\text{LCAO}}$ . To characterize the excited state by observables we define two matrices<sup>29</sup>

$$\begin{aligned} Q_{\mu\nu}^{(n)} &= \frac{1}{\sqrt{2}} \sum_{\substack{a \in \text{unocc} \\ i \in \text{occ}}} C_{n,ai}^{\text{CI}} (c_{\mu i}^{\text{LCAO}} c_{\nu i}^{\text{LCAO}} + c_{i\mu}^{\text{LCAO}} c_{i\nu}^{\text{LCAO}}) \\ P_{\mu\nu}^{(n)} &= \frac{i}{\sqrt{2}} \sum_{\substack{a \in \text{unocc} \\ i \in \text{occ}}} C_{n,ai}^{\text{CI}} (c_{\mu i}^{\text{LCAO}} c_{\nu i}^{\text{LCAO}} - c_{i\mu}^{\text{LCAO}} c_{i\nu}^{\text{LCAO}}) \end{aligned} \quad (1)$$

For site-representation of the CEO coordinate and momentum,<sup>30</sup> we define

$$\bar{Q}_{AB}^{(n)^2} = \sum_{\substack{\mu \in A \\ \nu \in B}} |Q_{\mu\nu}^{(n)}|^2 \quad \text{and} \quad \bar{P}_{AB}^{(n)^2} = \sum_{\substack{\mu \in A \\ \nu \in B}} |P_{\mu\nu}^{(n)}|^2 \quad (2)$$

Thus  $\bar{P}_{AB}^{(n)^2}$  gives the atomic sites A and B where the electron and the hole oscillate from and to, while  $\bar{Q}_{AB}^{(n)^2}$  is a measure of the delocalization of the exciton as a whole.

In real-space analysis the oscillating CEO coordinate and momentum are given as<sup>30</sup>

$$\begin{aligned} Q_n(r, r'; t) &= \sum_{\mu\nu} \phi_{\mu}^{\text{AO}}(\mathbf{r}) Q_{\mu\nu}^{(n)} \phi_{\nu}^{\text{AO}}(r') \cos(\omega_n t) \\ P_n(r, r'; t) &= \sum_{\mu\nu} \phi_{\mu}^{\text{AO}}(r) P_{\mu\nu}^{(n)} \phi_{\nu}^{\text{AO}}(r') \sin(\omega_n t) \end{aligned} \quad (3)$$

If the diagonal slice for  $\mathbf{r} = \mathbf{r}'$  in eq 3, the amplitude of the former is given by the so-called transition density (TD)

$$\rho_{n_0}(r) = \frac{1}{\sqrt{2}} \sum_{\mu, \nu} \phi_{\mu}^{\text{AO}}(r) Q_{\mu\nu}^{(n)} \phi_{\nu}^{\text{AO}}(r) \quad (4)$$

The TD contains information about the spatial location of the excitation and is directly related to the transition dipole. The charge difference density (CDD) is described as<sup>31–35</sup>

$$\Delta \rho_{nn}(\mathbf{r}) = 2i \sum_{\mu, \nu, \kappa} \phi_{\mu}^{\text{AO}}(r) Q_{\kappa\mu}^{(n)} P_{\kappa\nu}^{(n)} \phi_{\nu}^{\text{AO}}(r) \quad (5)$$

It represents the difference of electron distribution between the excited state  $|S_n\rangle$  and the ground state  $|S_0\rangle$ .

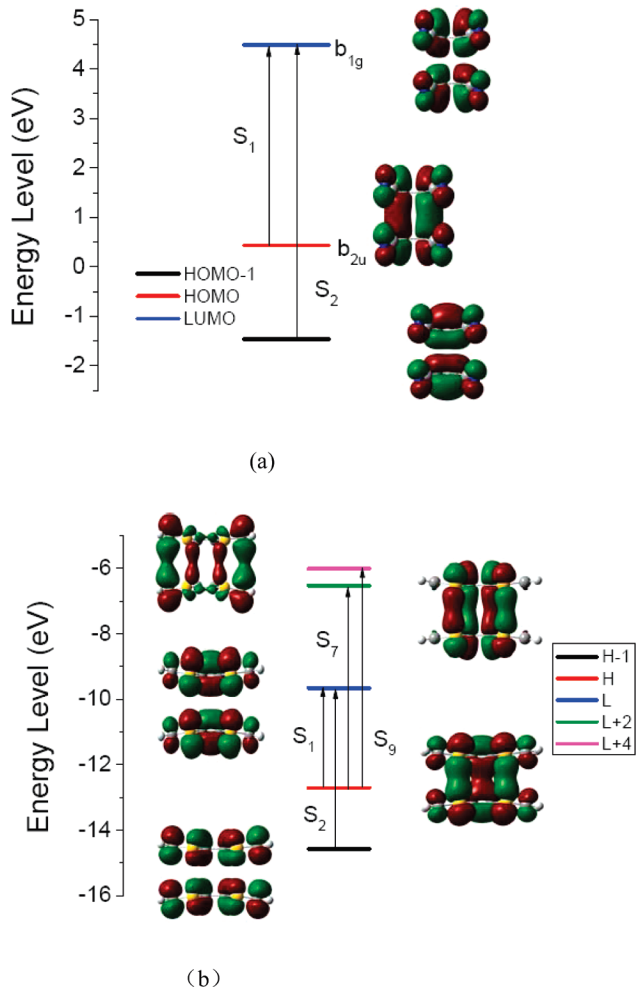


**Figure 1.** The energy levels and density distribution for the molecular orbitals, where a and b denote dianionic TCNE and dicationic TTF dimers, respectively. The green and red colors stand for different phase functions.

## III. Results and Discussion

**A. Ground-State Properties of Dianionic TCNE and Dicationic TTF Dimers.** For dianionic TCNE dimer, the crystallographically determined structures including  $[\text{TCNE}]_2^{2-}$  shows that intermonomer separation is  $2.89 \pm 0.06 \text{ \AA}^{11}$  (cal 2.8 Å), and this intriguing C–C separation is too short for a van der Waals complex but astonishingly long for a C–C bond, which may represent an emerging class of organic molecules that possess unusually long C–C bonding interactions.<sup>21</sup> From the viewpoint of molecular orbitals, this structure character is due to the fact that the electron cloudy overlap of the monomers produces the bonding HOMO of  $\pi$ -dimer, with  $b_{2u}$  symmetry. Figure 1a shows the energy levels and electron density distributions of the highest occupied molecular orbital (HOMO) and the lowest unoccupied molecular orbital (LUMO). Indeed, there are strong bonding interactions in the HOMO between the two TCNE<sup>−</sup> monomers. It is worth noting that these four-center two-electron  $\pi$ -bonding interactions also help to allow the TCNE monomers to come well inside the usual van der Waals envelope by partly compensating repulsive Coulomb and exchange interactions between filled orbitals that are responsible for normal van der Waals separations.<sup>21</sup> While for the antibonding LUMO of the dimer, the electron density exhibits the localized feature (in the monomers), and thus the state composed of HOMO–LUMO transition is viewed as a pattern of transition state associated with the electron transfer process.

**TABLE 1: Transition Energies and Oscillator Strengths for the Lowest 10 Singlet Excited States of Dianionic TCNE and Dicationic TTF Dimers**

	dianionic TCNE dimer			dicationic TTF dimer		
	E (nm)	f	exp (nm) <sup>a</sup>	E (nm)	f	exp (nm) <sup>b</sup>
S <sub>1</sub>	<b>482.12</b>	<b>0.4419</b>	528	<b>739.98</b>	<b>0.3280</b>	717
S <sub>2</sub>	<b>316.22</b>	<b>0.3350</b>		<b>452.20</b>	<b>0.1372</b>	
S <sub>3</sub>	308.82	0.0126		363.51	0.0000	
S <sub>4</sub>	296.42	0.0000		352.71	0.0000	
S <sub>5</sub>	283.80	0.0000		334.78	0.0003	
S <sub>6</sub>	281.35	0.0003		318.61	0.0000	
S <sub>7</sub>	245.42	0.0000		<b>306.88</b>	<b>0.5072</b>	
S <sub>8</sub>	242.32	0.0000		301.33	0.0219	
S <sub>9</sub>	236.66	0.0000		<b>278.94</b>	<b>0.0883</b>	
S <sub>10</sub>	227.26	0.0000		260.92	0.0000	

<sup>a</sup> Reference 16. <sup>b</sup> Reference 13.

The electronic coupling element ( $H_{ab}$ ) in the electron transfer process, which implies the particular pair of states (the initial and final states), can be calculated according to the generalized Mulliken-Hush (GMH) model.<sup>18</sup> In the two-state ( $S_0$  and  $S_1$  states) formulation

$$H_{ab} = \frac{\mu_{tr}\Delta E}{\sqrt{(\Delta\mu)^2 + 4(\mu_{tr})^2}} \quad (6)$$

where  $\mu_{tr}$  is the calculated transition dipole moment,  $\Delta\mu$  is the dipole moment difference between the two states, and  $\Delta E$  is the vertical excitation energy, and all dipole quantities are vector components in the charge-transfer direction, which will be discussed later).  $\Delta\mu$  in eq 6 can be estimated by using a finite field method on the excitation energy. The transition energy dependent on the static electric field  $F$  can be expressed as<sup>40</sup>

$$E_{exc}(F) = E_{exc}(0) - \Delta\mu F - \frac{1}{2}\Delta\alpha F^2 \quad (7)$$

where  $E_{exc}(0) = \Delta E$  is the excitation energy at zero field,  $\Delta\alpha$  is the change in polarizability. The fitted value of  $\Delta\mu$  is 0.01667 au, and the electronic coupling element ( $H_{ab}$ ) is calculated to be the value of 0.047 au (1279 meV). The large value of  $H_{ab}$  in the dimer system indicates the strong electron coupling between two states, and the fast electron transfer easily takes place according to Fermi's Golden rule.<sup>41</sup>

For dicationic TTF dimer, cofacial configuration was reported<sup>14</sup> and intermonomer separation 3.40 Å (cal 3.43 Å). The energy levels and electron density distributions of HOMO-1, HOMO, LUMO, LUMO+2 and LUMO+4 are shown in Figure 1b, in which active orbitals are directly related to the electron transition of main absorption. As shown in Figure 1b, the two TTF monomers have strong bonding interactions, and in HOMO electron density is spatially distributed between the two monomers. The fitted  $\Delta\mu = 0.071$  au, and  $H_{ab} = 0.037$  au (1007 meV).

**B. Optical Absorption Spectra of Dicationic TTF and Dianionic TCNE Dimers.** The results of low-lying electronic transitions obtained at the TDDFT-CAM-B3LYP/6-31G(d) level of theory are summarized in Table 1. The simulated absorption spectra of dicationic TTF and dianionic TCNE are shown in Figure 2. For dicationic TTF and dianionic TCNE, the dominant orbital contribution to the electronic excitation originates from the HOMO to the LUMO transition, as shown in Figure 1.

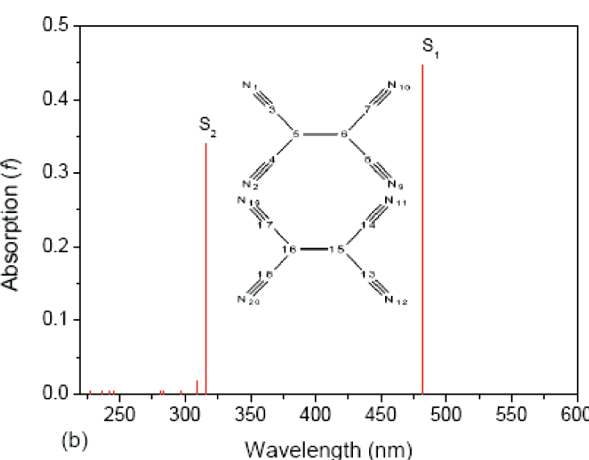
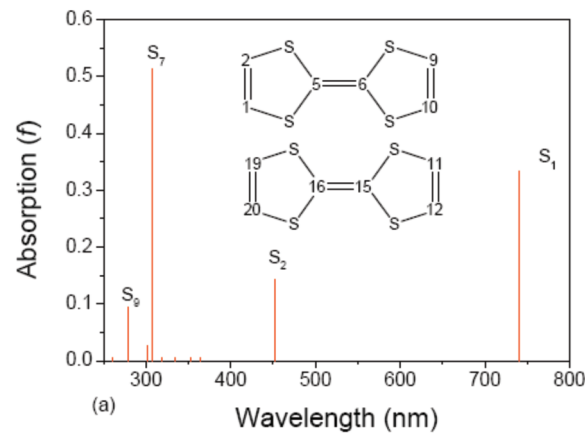


**Figure 2.** The calculated absorption spectrum of (a) dicationic TTF and (b) dianionic TCNE dimers.

Calculated lowest energy excited state of dicationic TTF is found to be 739.98 nm (experimental 717 nm) with dipole-allowed electron transition, and one of dianionic TCNE is located at 482.12 nm (experimental 528 nm). The simulated UV-vis spectra are in good agreement with the experimental reports.<sup>13,16</sup> For dicationic TTF, other states with large oscillator strength ( $f \geq 0.01$ ) correspond to  $S_2$ ,  $S_7$ , and  $S_9$  states, respectively. While for dianionic TCNE, another absorption peak is  $S_2$  state. The excited states properties mentioned above will be further explored by the two-dimensional (2D) site (transition density matrix) and the three-dimensional (3D) cube (transition density and charge difference density) representations as below.

**C. Charge-Transfer and Electron–Hole Coherence for Dicationic TTF Dimer.** To reveal charge-transfer and electron–hole coherence for dicationic TTF dimer, we use site-representation of the CEO coordinate and momentum ( $\bar{Q}_{AB}^{(n)2}$  and  $\bar{P}_{AB}^{(n)2}$ ). Upon photon-excitation, electron density of atomic sites A and B of dimer undergoes redistribution, and  $\bar{P}_{AB}^{(n)2}$  describes where electron and hole oscillate and where they come from and go to (i.e., the contribution of atomic sites to the production of electron and hole), and  $\bar{Q}_{AB}^{(n)2}$  is a measure of the delocalization of the exciton. The contour plots of  $|Q|^2$  and  $|P|^2$  of the four absorption peaks can be seen from Figure 3, where the number of atoms and monomer region (1 and 2 units) are labeled to clearly indicate the excited-state dynamics behavior. As shown  $|Q|^2$  in Figure 3, the exciton (along the diagonal elements) for dicationic TTF  $S_1$  state is within the monomers since the electron–hole pair are localized in 1 and 2 units, respectively, and thus for this state there is no coupling exciton (the coupling constant ( $M$ ) of exciton between the monomers is close to zero). The

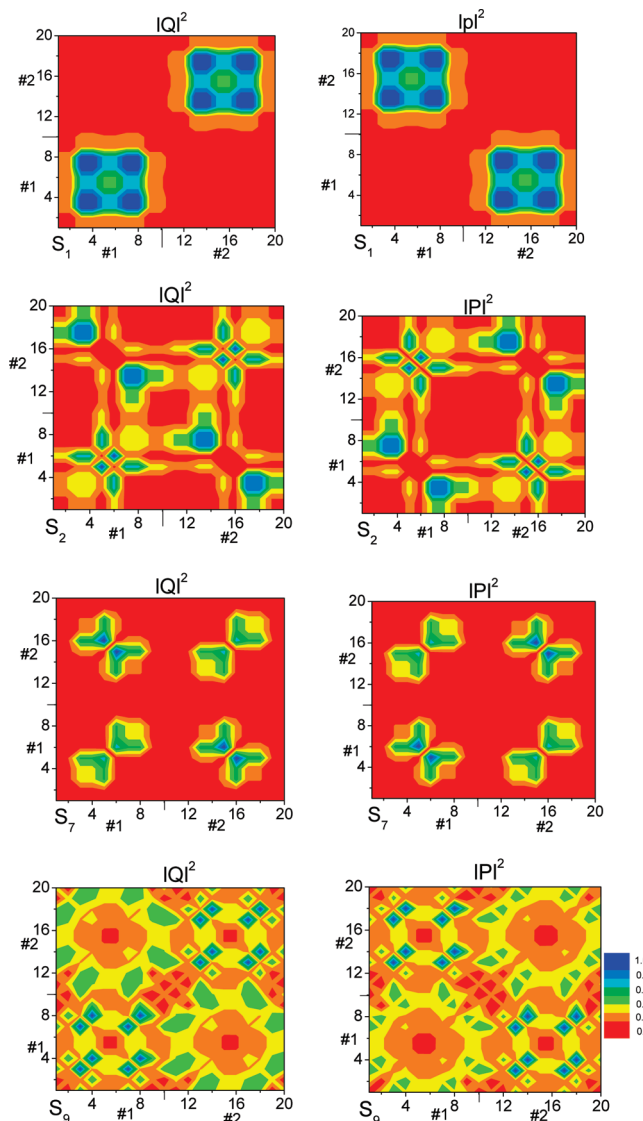


**Figure 3.** The contour plots of 2D site representation (transition density matrix) for dicationic TTF, in which the two units (1 and 2) represent the two monomers and the number of atoms along coordinate axes can be seen from the Figure 2a.

whole term of  $|Q|^2$  is written as  $|Q_1|^2 = |Q_1(a)|^2 + |Q_1(b)|^2$ . In the case of the oscillation of electron–hole, it occurs between the monomers (see  $|P|^2$  plot of  $S_1$ , along the off-diagonal elements), which indicates that the coupling constant ( $N$ ) of oscillation of electron–hole pairs is not zero, and more detailed  $|P_1|^2 = |P_1(a,b)|^2$ , since there is no oscillation of electron–hole pairs within the monomers ( $|P_1(a)|^2 = |P_1(b)|^2 = 0$ ).

The reason why the electron–hole pairs oscillate between the monomers can be interpreted with transition density, which reveals the orientation and the strength of transition dipole moment (where the green and red stand for the hole and electron densities, respectively.). As shown in Figure 4, the oscillation takes place between the two monomers, and transition dipole moment displays a singlet orientation, i.e., this orientation is from the electron density mainly resided in the above monomer to the hole density of the below one. This transition density well reflects the transition dipole moment characteristics during photoexcitation, and the corresponding calculated transition dipole moments are listed in Table 2, where the Cartesian coordinate of them is also shown. The CDD (see Figure 5) allows us to follow the change of the static charge distribution

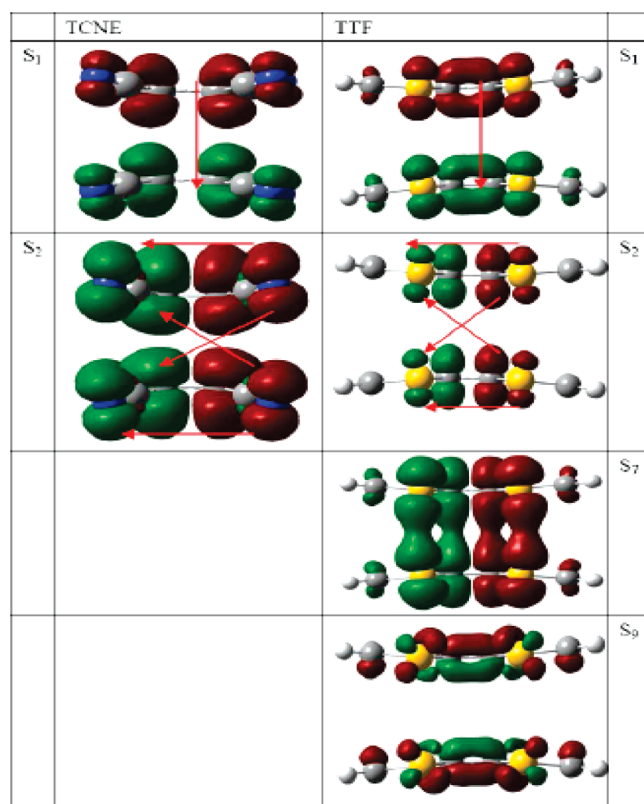


**Figure 4.** The TD for the strong absorption peaks in Figure 2, where the green and red stand for the hole and electron densities, respectively.

upon excitation. From charge difference density of  $S_1$ , it is found that most of the extra positive charges are localized in the space between the two monomers.

Different from the  $S_1$  state,  $S_2$  state exhibits strong coupling effects between the two monomers. From the  $|Q_2|^2$  and  $|P_2|^2$  of  $S_2$  state in Figure 3, the exciton and the oscillation of electron–hole pairs occur not only within the two monomers but also between the monomers (along the diagonal and off-diagonal elements), which indicates that the coupling constants ( $M$  and  $N$ ) of exciton and oscillation of electron–hole pairs are nonzero, and there exists strongly coupling effects between the monomers for  $S_2$  state. Upon photon-excitation, those strong coupling effects are attributed to the coaction of two kinds of transition dipole moments: (a) the one is the intramonomer transition dipole moments from side to side (see Figure 4) and (b) the other one belongs to the intermonomer transition dipole moments. However, the whole of transition dipole moments maintains the orientation of  $x$  axes, as is supported with the calculated transition dipole moments in Table 2. From the charge difference density in Figure 5, the extra positive charges reside at the edge of the monomers, and the electrons are localized in the center of the monomers. It is understandable that the intermonomer transition dipole moments result in the exchange of electron–hole pairs between the monomers (see Figure 3, contour plot  $|P_2|^2$ ).

Similarly, for  $S_7$  and  $S_9$  states they also have strong coupling of the exciton and the oscillation of electron–hole pairs between the monomers (see Figure 3). From charge difference density of  $S_7$  in Figure 5, there is stronger localization of electrons in the central space of the two monomers. From the viewpoint of electron transition,  $S_7$  state has major contributions from HOMO  $\rightarrow$  LUMO+2 electron transition, which involves the

**TABLE 2: Calculated Transition Dipole Moments for Dianionic TCNE and Dicationic TTF Dimers also with the Cartesian Coordinates**

	X (au)	Y (au)	Z (au)	X (au)	Y (au)	Z (au)
<b>S<sub>1</sub></b>	-0.0120	-2.6482	0.0170	0.0008	-2.8269	0.0004
<b>S<sub>2</sub></b>	-1.8674	0.0082	0.0021	-1.4294	0.0000	-0.0001
<b>S<sub>7</sub></b>				-2.2636	-0.0006	-0.0001
<b>S<sub>9</sub></b>				0.0002	-0.0005	0.9004

localized excitation from the edge of the monomer to center C atoms and electron delocalization in the center space of the two monomers.

**D. Charge-Transfer and Electron–Hole Coherence for the Dianionic TCNE Dimer.** The contour plots of  $|Q_1|^2$  and  $|P_1|^2$  at the two absorption peaks can be seen from Figure 6. Obviously, the exciton for  $S_1$  is within the monomers, so the coupling constant  $M = 0$ , and  $|Q_1(a,b)|^2 = 0$ . Meanwhile, the oscillation of electron–hole pairs takes place between the monomers (the coupling constant  $N \neq 0$ ), that is, there is no oscillation of electron–hole within the monomers ( $|P_1(a)|^2 = |P_1(b)|^2 = 0$ ), and the transition moments for this state is characterized as one direction transition moment from one

monomer to another (see Figure 4 and data in Table 2). For the dianionic TCNE dimer  $S_1$  state (the corresponding strongest absorption), the transition moment properties has similar trend as that of dicationic TTF  $S_1$  state. It is worth noting that for dicationic TTF, the strongest absorption is located at the  $S_7$  state corresponding to the strong coupling effects between the monomers. Charge transfer (see Figure 5) exhibits different dynamic process, i.e., for dianionic TCNE all of the electrons are localized in the two monomer, and the positive charges are localized in the space between the monomers; while for dicationic TTF, the electron density moves to the central space between the two monomers.

For the dianionic TCNE dimer  $S_2$  state, Figure 6 shows that the exciton and the oscillation of electron–hole pairs occur not only within the monomers but also between the monomers, which indicates that the coupling constants  $M \neq 0$  and  $N \neq 0$ . It is due to the fact that there are four transition dipole moments, two of which are intramonomer transition dipole moments, and the others are intermonomer transition dipole moments (see TD in Figure 4). From charge difference density in Figure 6, the positive charges reside in two central C–C bonds and eight

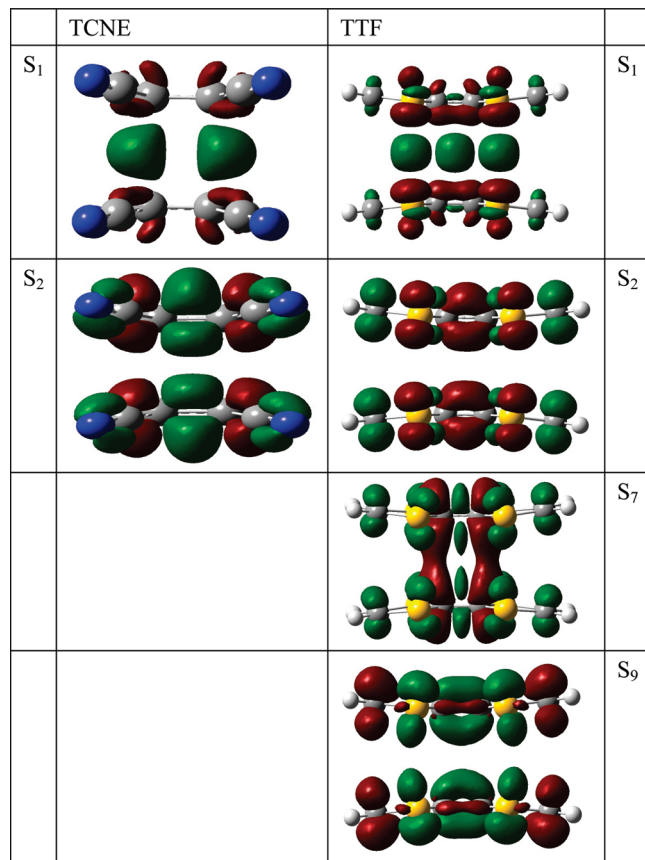


**Figure 5.** The CDDs for the strong absorption peaks in Figure 2, where the green and red stand for the hole and electron densities, respectively.

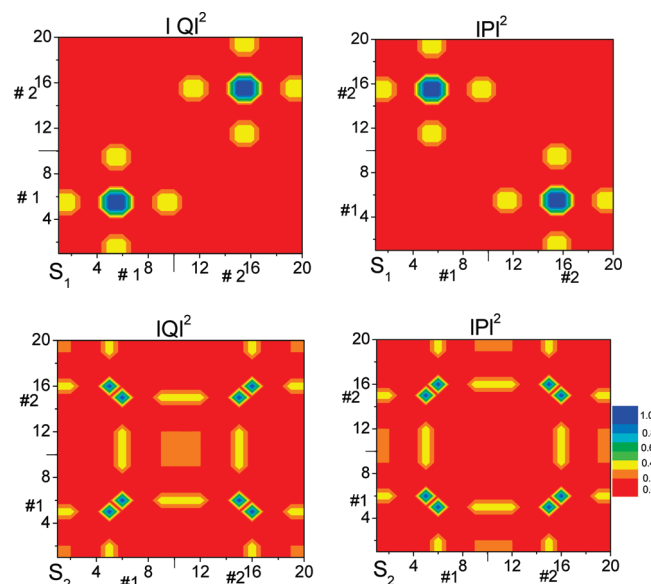


**Figure 6.** The contour plots of 2D site representation (transition density matrix) for dianionic TCNE, in which the two units (1 and 2) represents the two monomers and the number of atoms along coordinate axes can be seen from the Figure 2b.

$\text{C}\equiv\text{N}$  bonds at the edge, and the electrons are localized in other eight C—C bonds.

#### IV. Conclusion

The study of dianionic TCNE and dicationic TTF dimers is an interesting subject for special optical physics properties and function as molecular materials. A better understanding of the excited behavior of the charge  $\pi$ -dimers and the coupling effect between the two monomers will help the rational design efforts in these areas. The absorption of dianionic TCNE and dicationic TTF dimers have been calculated by TD-CAM-B3LYP, which functional combine the hybrid qualities of B3LYP and the long-range correction, and the calculated results (the main absorption peaks) have been identified with the visualized 2D site of transition density matrix and the 3D cube representations of charge different density and transition density. The 2D site and 3D cube representations reveal that the strongest absorption ( $S_7$ ) of dicationic TTF can be produced through the mixture of intermolecular and intramolecular CT process, followed by the strong coupling effect (coupling constants  $M \neq 0$  and  $N \neq 0$ ). A similar trend is found upon secondary absorption band of dianionic TCNE, namely, there exists simultaneous mixture charge-transfer process. While for the strongest absorption ( $S_1$ ) of dianionic TCNE, the exciton resides within the monomers displaying coupling constant of exciton ( $M = 0$ ), while the electron and the hole oscillate between the monomers with nonzero coupling constant of oscillation ( $N$ ). This state is characterized as an intermolecular charge transfer excited state. Almost all holes are localized in the middle area of  $\pi$ -dimers and the electrons on the  $\pi$ -dimer backbones, evidenced by the visualized 3D charge different densities analysis.

**Acknowledgment.** This work was supported by the National Natural Science Foundation of China (Grant Nos. 10604012, 10974023, 10874234, 20703064, and 90923003).

#### References and Notes

- (1) Muller-Dethlefs, K.; Hobza, P. *Chem. Rev.* **2000**, *100*, 143.
- (2) Kim, K. S.; Tarakeshwar, P.; Lee, J. Y. *Chem. Rev.* **2000**, *100*, 4145.
- (3) Devic, T.; Yuan, M.; Adams, J.; Fredrickson, D. C.; Lee, S.; Venkataraman, D. *J. Am. Chem. Soc.* **2005**, *127*, 14616.
- (4) Santoro, F.; Barone, V.; Improta, R. *Proc. Natl. Acad. Sci. U.S.A.* **2007**, *104*, 9931.
- (5) Gregg, B. A.; Kose, M. E. *Chem. Mater.* **2008**, *20*, 5235.
- (6) Garcia-Yoldi, I.; Mota, F.; Novoa, J. J. *J. Comput. Chem.* **2007**, *28*, 326.
- (7) (a) Zhou, H.; Wong, N. B.; Lau, K. C.; Tian, A.; Li, W. K. *J. Phys. Chem. A* **2007**, *111*, 9838. (b) Leitch, A. A.; Reed, R. W.; Robertson, C. M.; Britten, J. F.; Yu, X. Y.; Secco, R. A.; Oakley, R. T. *J. Am. Chem. Soc.* **2007**, *129*, 7903.
- (8) Sun, M. T.; Pullerits, T.; Kjellberg, P.; Beenken, W. J. D.; Han, K. L. *J. Phys. Chem. A* **2006**, *110*, 6324.
- (9) Distasio, R. A.; von Helden, G.; Steele, R. P.; Head-Gordon, M. *Chem. Phys. Lett.* **2007**, *437*, 277.
- (10) Rosokha, S. V.; Kochi, J. K. *J. Am. Chem. Soc.* **2007**, *129*, 3683.
- (11) (a) Fox, J. R.; Foxman, B. M.; Guarnera, D.; Miller, J. S.; Calabrese, J. C.; Reis, A. H. *J. Mater. Chem.* **1996**, *6*, 1627. (b) Johnson, M. T.; Campana, C. F.; Foxman, B. M.; Desmarais, W.; Vela, M. J.; Miller, J. S. *Chem.—Eur. J.* **2000**, *6*, 1805.
- (12) Miller, J. S.; Novoa, J. J. *Acc. Chem. Res.* **2007**, *40*, 189.
- (13) Torrance, J. B.; Scott, B. A.; Welber, B.; Kaufman, F. B.; Seiden, P. E. *Phys. Rev. B* **1979**, *19*, 730.
- (14) (a) Yakushi, K.; Nishimura, S.; Sugano, T.; Kuroda, H.; Ikemoto, I. *Acta Crystallogr., Sect. B* **1980**, *36*, 358. (b) Rosokha, S. V.; Newton, M. D.; Jalilov, A. S.; Kochi, J. K. *J. Am. Chem. Soc.* **2008**, *130*, 1944.
- (15) Khodorkovsky, V.; Shapiro, L.; Krief, P.; Shames, A.; Mabon, G.; Gorgues, A.; Giffard, M. *Chem. Commun.* **2001**, 2736.
- (16) Del Sesto, R. E.; Miller, J. S.; Lafuente, P.; Novoa, J. J. *Chem.—Eur. J.* **2002**, *8*, 4894.
- (17) Jakowski, J.; Simons, J. *J. Am. Chem. Soc.* **2003**, *125*, 16089.
- (18) Wang, Q.; Newton, M. D. *J. Phys. Chem. B* **2008**, *112*, 568.
- (19) Novoa, J. J.; Lafuente, P.; Del Sesto, R. E.; Miller, J. S. *Angew. Chem., Int. Ed. Engl.* **2001**, *40*, 2540.
- (20) Clark, A. E.; Qin, C. Y.; Li, A. D. Q. *J. Am. Chem. Soc.* **2007**, *129*, 7586.
- (21) Jung, Y. S.; Head-Gordon, M. *Phys. Chem. Chem. Phys.* **2004**, *6*, 2008.
- (22) Garcia-Yoldi, I.; Miller, J. S.; Novoa, J. J. *J. Phys. Chem. A* **2007**, *111*, 8020.
- (23) Li, Z. J.; Wang, F. F.; Li, Z. R.; Xu, H. L.; Huang, X. R.; Wu, D.; Chen, W.; Yu, G. T.; Gu, F. L.; Aoki, Y. *Phys. Chem. Chem. Phys.* **2009**, *11*, 402.
- (24) Pan, F.; Gao, F.; Liang, W. Z.; Zhao, Y. *J. Phys. Chem. B* **2009**, *113*, 14581.
- (25) Garcia-Yoldi, I.; Miller, J. S.; Novoa, J. J. *J. Phys. Chem. A* **2009**, *113*, 7124.
- (26) Santoro, F.; Barone, V.; Improta, R. *J. Am. Chem. Soc.* **2009**, *131*, 15232.
- (27) Chakrabarti, S.; Ruud, K. *J. Phys. Chem. A* **2009**, *113*, 5485.
- (28) Kuhlman, T. S.; Mikkelsen, K. V.; Moller, K. B.; Soling, T. I. *Chem. Phys. Lett.* **2009**, *478*, 127.
- (29) (a) Sun, M. T.; Kjellberg, P.; Beenken, W. J. D.; Pullerits, T. *Chem. Phys.* **2006**, *327*, 474. (b) Sun, M. T. *J. Chem. Phys.* **2006**, *124*, 054903.
- (30) (a) Tretiak, S.; Mukamel, S. *Chem. Rev.* **2002**, *102*, 3171. (b) Mukamel, S.; Tretiak, S.; Wagersreiter, T.; Chernyak, V. *Science* **1997**, *277*, 781.
- (31) (a) Jespersen, K. G.; Beenken, W. J. D.; Zaushitsyn, Y.; Yartsev, A.; Andersson, M.; Pullerits, T.; Sundstrom, V. *J. Chem. Phys.* **2004**, *121*, 12613. (b) Sun, M. T.; Ding, Y.; Xu, H. X. *J. Phys. Chem. B* **2007**, *111*, 13266.
- (32) Beenken, W. J. D.; Pullerits, T. *J. Phys. Chem. B* **2004**, *108*, 6164.
- (33) Sun, M. T.; Liu, L.; Ding, Y.; Xu, H. X. *J. Chem. Phys.* **2007**, *127*, 084706.
- (34) Liu, S. S.; Zhao, X. M.; Li, Y. Z.; Chen, M. D. *J. Chem. Phys.* **2009**, *130*, 234509.
- (35) Sun, M. T.; Xu, H. X. *ChemPhysChem* **2009**, *10*, 392.
- (36) Dreizler, M. R. G., E.K.U. Density Functional Theory; Springer-Verlag: Heidelberg, 1990.
- (37) Stratmann, R. E.; Scuseria, G. E.; Frisch, M. J. *J. Chem. Phys.* **1998**, *109*, 8218.
- (38) Yanai, T.; Tew, D. P.; Handy, N. C. *Chem. Phys. Lett.* **2004**, *393*, 51.
- (39) Frisch, M. J. T.; Trucks, G. W.; Schlegel, H. B.; Scuseria, G. E.; Robb, M. A.; Cheeseman, J. R.; Scalmani, G.; Barone, V.; Mennucci, B.; Petersson, G. A.; Nakatsuji, H.; Caricato, M.; Li, X.; Hratchian, H. P.; Izmaylov, A. F.; Bloino, J.; Zheng, G.; Sonnenberg, J. L.; Hada, M.; Ehara, M.; Toyota, K.; Fukuda, R.; Hasegawa, J.; Ishida, M.; Nakajima, T.; Honda, Y.; Kitao, O.; Nakai, H.; Vreven, T.; Montgomery, J. A., Jr.; Peralta, J. E.; Ogliaro, F.; Bearpark, M.; Heyd, J. J.; Brothers, E.; Kudin, K. N.; Staroverov, V. N.; Kobayashi, R.; Normand, J.; Raghavachari, K.; Rendell, A.; Burant, J. C.; Iyengar, S. S.; Tomasi, J.; Cossi, M.; Rega, N.; Millam, J. M.; Klene, M.; Knox, J. E.; Cross, J. B.; Bakken, V.; Adamo, C.; Jaramillo, J.; Gomperts, R.; Stratmann, R. E.; Yazyev, O.; Austin, A. J.; Cammi, R.; Pomelli, C.; Ochterski, J. W.; Martin, R. L.; Morokuma, K.; Zakrzewski, V. G.; Voth, G. A.; Salvador, P.; Dannenberg, J. J.; Dapprich, S.; Daniels, A. D.; Farkas, O.; Foresman, J. B.; Ortiz, J. V.; Cioslowski, J.; Fox, D. J. Gaussian 09; Gaussian, Inc.: Wallingford, CT., 2009.
- (40) Grozema, F. C.; Telesca, R.; Jonkman, H. T.; Siebbeles, L. D. A.; Snijders, J. G. *J. Chem. Phys.* **2001**, *115*, 10014.
- (41) (a) Mikkelsen, K. V.; Ratner, M. A. *Chem. Rev.* **1987**, *87*, 113. (b) Newton, M. D. *Chem. Rev.* **1991**, *91*, 767.